phys. stat. sol. (a) **191**, No. 2, 509–518 (2002)

Transport Properties of As-Prepared Al-Doped Zinc Oxide Films Using Sol–Gel Method

G. K. Paul, S. Bandyopadhyay, and S. K. Sen[1])

Department of Materials Science, Indian Association for the Cultivation of Science, Calcutta 700032, India

(Received August 7, 2001; in revised form March 11, 2002; accepted March 15, 2002)

Subject classification: 68.55.Jk; 71.55.Ht; 73.50.Gr

ZnO films doped with different concentrations of aluminum (AZO) have been prepared by the sol–gel technique. The electrical properties of the samples have been measured on as-deposited films. Two of the films have been heat treated in vacuum at 400 °C to determine the changes in transport properties. The electrical properties, i.e. conductivity and Hall coefficient, have been studied from room temperature down to low temperatures. Combining these two it has been possible to determine the Hall mobilities, carrier concentrations and the barrier height at the grain-boundary region. Attempts have been made to explain the barrier height assuming monovalent trapping states at the grain boundary and the density of trapped states has been estimated from the experimental data. As carrier concentration increases after heat treatment of the samples in vacuum the role of non-ionized impurities decreases.

1. Introduction

The increased application of transparent conducting oxide film as a conducting layer as well as one of the electrodes in modern solar cells is the motivation for the study of conducting ZnO films. These films are prepared by several processes like metal organic chemical vapor deposition [1, 2], dc or rf magnetron sputtering [3, 4], spray pyrolysis [5, 6] and the sol–gel process [7, 8]. The films prepared by different methods have large variations of resistivities and Hall coefficients. The cause is not well understood and well studied. On the other hand, the most well-studied semiconducting material is silicon. The electrical properties of polycrystalline silicon have been extensively investigated in terms of two models: segregation theory [9] and grain-boundary (g.b.) trapping theory [10]. According to segregation theory the atoms are electrically inactive whereas in the trapping theory carriers are captured at the trapping states at the g.b. The trapped charges create potential barriers opposing the carrier transport from one grain to other. The aim of this work is to study the temperature dependence of the electrical properties of sol–gel-derived aluminum-doped ZnO (AZO) film by varying the doping level, and to try to explain the data in terms of existing theories of grain-boundary segregation or trapping.

2. Experimental Procedure

The details of the preparation method of the films have already been described earlier [7]. Briefly, it is described below. Zinc acetate 2 hydrate (extra pure quality) was added in dehydrated isopropyl alcohol so as to prepare a concentration of 0.6 mol/l. The resul-

[1]) Corresponding author; Tel.: 91 33 473 4971; Fax: 91 33 473 2805;
e-mail: saurindras@hotmail.com

 0031-8965/02/19106-0509 $ 17.50+.50/0

tant solution was mixed thoroughly on a magnetic stirrer. After a time, it started turning milky. An equimolar quantity of extra pure diethanolamine (DEA) was introduced as a sol stabilizer drop-by-drop into the solution until it became transparent. $Al(NO_3)_3 \cdot 9\ H_2O$ was added as dopant. The films were prepared on thoroughly cleaned glass slides by a drain-coating method. The draining rate was about 6 cm/min.

The coated films were kept in a furnace at 120 °C in air for 30 min and then quickly transferred into another furnace at 550 °C and heated for 40 min in air. This process has been repeated ten times to prepare samples of almost the same thickness. Usually these films were heated in vacuum or in furnace in the presence of hydrogen or nitrogen [7, 8] to increase the conductivity of the samples by almost two orders of magnitude. In this study, as-prepared samples were investigated. The thickness and uniformity of film thickness were monitored using a surfometer. The films are uniform in thickness, average thickness being 540 nm. The structure and crystallinity of the films were analyzed by a X-ray diffractometer (Philips model PW1730) using CuK_α radiation. The experiments were carried out on four Al-doped samples in the proportion of 0.7, 1, 1,7, and 2 at%. The microstructure of one of the samples (1 at%) investigated in a Leo S43DI scanning electron microscope (SEM) is quoted for average grain-size determination.

The electrical conductivity, the carrier concentration and Hall mobility of the films were measured by the van der Pauw four-probe technique with a square configuration in the temperature range of 130–300 K. The four contacts each having an area of about 0.01 cm^2, were realized with gold deposition. Good Ohmic contact between electrode

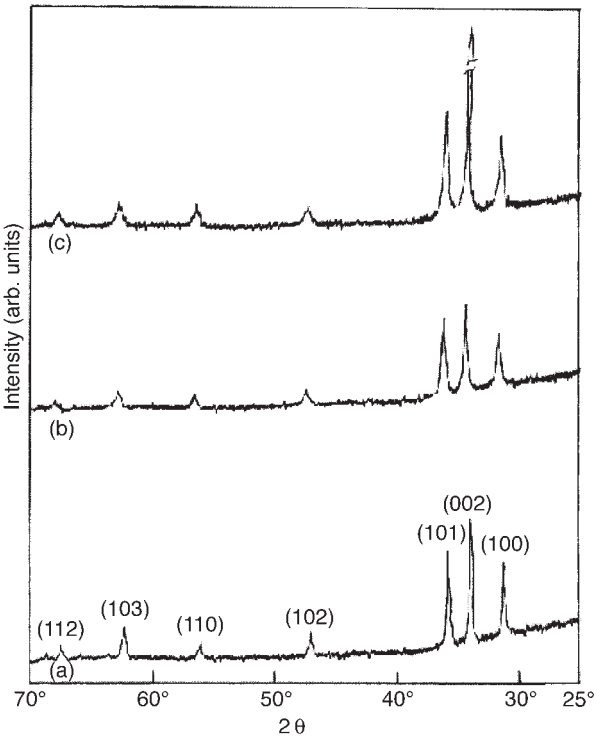

Fig. 1. XRD patterns of a) 0.7; b) 1.0; c) 2.0 at% aluminum-doped ZnO film

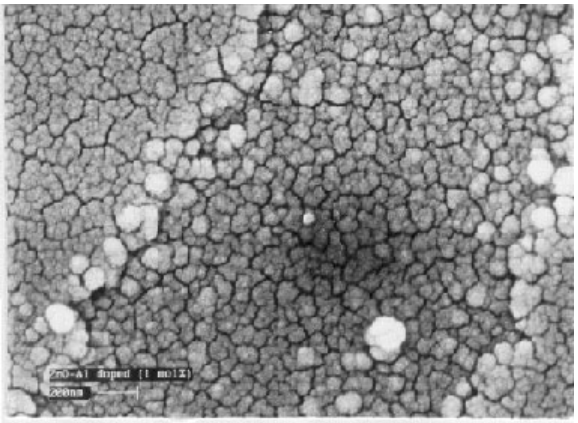

Fig. 2. SEM of 1 at% aluminum-doped sample

and ZnO films was confirmed before measurements were taken. The measurements for Hall effect were carried out utilizing a magnetic field of 5 kG and the substrate area (2 cm^2) in this measurement was much lower than the area around the pole pieces of the magnet. Low temperature was attained in a controlled cryostat using liquid nitrogen.

3. Results and Discussion

The X-ray diffraction (XRD) patterns of three of the doped films (0.7, 1.0, and 2.0 at%-doped) are shown in Fig. 1. They indicate that the films are polycrystalline in nature with a tendency for orientation along the 002 direction. The crystalline sizes vary from 15–20 nm. There is no remarkable change in crystallinity and crystalline size with doping but a slight gradual shift of the peaks to the higher angle side has been observed. This indicates an increase in lattice strain with doping. The scanning electron micrograph (SEM) of the 1 at%-doped sample (Fig. 2) indicates that the average grain size is of the order of 40 nm.

Hall and electrical resistivity measurements of the samples prepared at the same conditions, i.e. the same annealing temperature (550 °C), but having different doping concentrations of aluminum (0.7 to 2 at%) were made. Both the measurements were performed simultaneously. We could not observe any typical hysteresis in Hall measurements at any temperatures where measurements were done. The results are

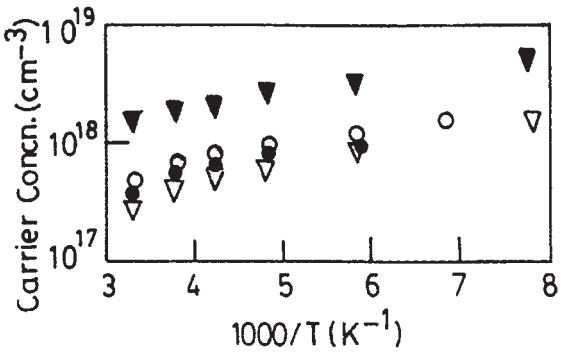

Fig. 3. Plot of carrier concentration against reciprocal of temperature (▽ 0.7 at%, ● 1 at%, ▼ 1.7 at%, ○ 2.0 at%)

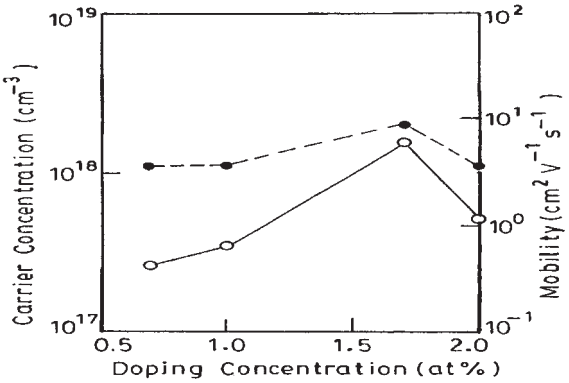

Fig. 4. Plot of carrier concentration (○) and mobility (●) against doping concentration

presented below in terms of carrier concentration, mobility and electrical resistivity of different doped samples.

3.1 Hall measurements

In Fig. 3 the plot of carrier concentration (n) against inverse of temperature is shown for four as-deposited samples having different doping concentration (n_d). It is seen that there is a very small but consistent increase in n as temperature decreases. The carrier concentration of all the samples is always several orders less than the doping concentration. For example, the calculated doping concentration of 1 at% aluminum-doped ZnO film is about $4 \times 10^{20}\,\mathrm{cm}^{-3}$ but the carrier concentration is $3.4 \times 10^{17}\,\mathrm{cm}^{-3}$ at room temperature, which is about three orders less. Figure 4 indicates that both the carrier concentration and Hall mobility measured at room temperature initially increase with doping reaching maximum at 1.7 at%-doped sample and then decrease. As a result, the resistivity of that particular film has been found to be minimum. We have already mentioned that in most of the earlier publications the films have been further annealed in high vacuum or hydrogen or nitrogen atmospheres to reduce the resistivity by at least two to three orders of magnitude. Otherwise, the resistivities of as-deposited samples [7] are of the same order of magnitude as found by us. However, on heating two of our samples at 400 °C in high vacuum for 30 min the resistivities were lowered (Table 1) and they become comparable to the values quoted in earlier works.

3.2 Electrical resistivity measurements

Figures 5 and 6 indicate the change in mobility (μ) and resistivity (ϱ), respectively, against reciprocal of temperature. The Hall mobility in all cases decreases with decrease in temperature.

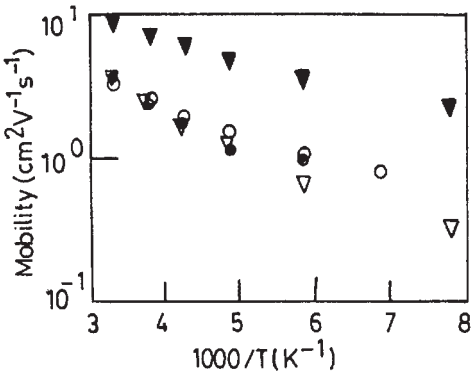

Fig. 5. Plot of mobility against reciprocal of temperature (▽ 0.7 at%, ● 1 at%, ▼ 1.7 at%, ○ 2.0 at%)

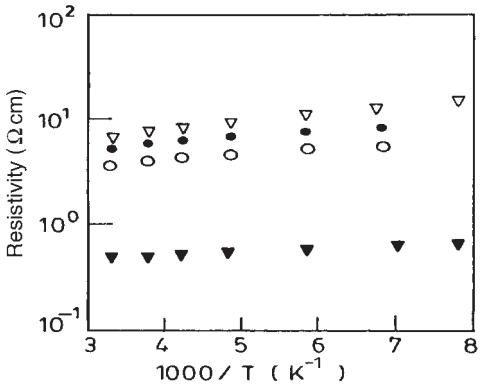

Fig. 6. Plot of resistivity (ϱ) against reciprocal of temperature (▽ 0.7 at%, ● 1 at%, ▼ 1.7 at%, ○ 2.0 at%)

There are several conduction models in the literature to explain the temperature dependence of conductivity in polycrystalline films. The basic model was proposed by Volger [11] and Petriz [12] and the refinements were done by Orton and Powell [13] and Seto [10]. A polycrystalline film can be thought to be composed of grains with a grain boundary (g.b.) in between. Generally, the g.b. contains a large amount of surface trapping states that can trap free carriers from the bulk material. This results in a band bending near the g.b. and a depletion region near the boundary. Thus, the boundary region can be described electrically in terms of two back-to-back Schottky barriers through which the charge carrier transport takes place by thermionic emission. The conductivity σ_{th} in such cases are given by

$$\sigma_{\text{th}} = [Le^2 n/(2\pi m^* kT)^{1/2}] \exp(-E_{\text{B}}/kT)\,, \tag{1}$$

where n is the carrier concentration, m^* the effective mass and k the Boltzmann constant, E_{B} is the barrier height and L is crystallite size.

This is the starting point for interpreting the conductivity temperature data. The contribution to the conductivity is thermally activated with a barrier height E_{B} determined by the band-edge mismatch and the position of the Fermi level.

Equation (1), which can be written as

$$\sigma = en\mu_0 T^{-1/2} \exp(-E_{\text{B}}/kT)\,, \tag{2}$$

where

$$\mu_0 = Le/(2\pi m^* k)^{1/2} \tag{3}$$

has been approximated as

$$\sigma = en\mu\,, \tag{4}$$

where the mobility is

$$\mu = \mu_0 T^{-1/2} \exp(-E_{\text{B}}/kT)\,. \tag{5}$$

The barrier height can be obtained from the slope of the ln ($\mu T^{1/2}$) against $1/T$ curve. Such curves are shown in Fig. 7. The slopes of the curves are different in the high- and low-temperature regions. The high-temperature region corresponds to thermionic emission, whereas the variation in the low-temperature region might be due to other pro-

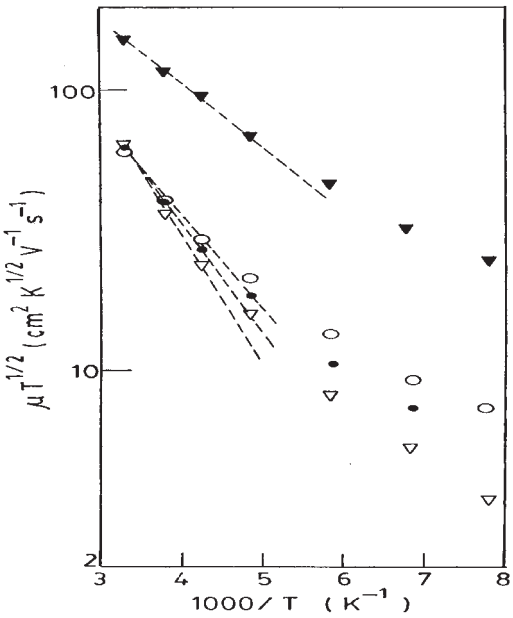

Fig. 7. Plot of $\mu T^{1/2}$ against reciprocal of temperature (▽ 0.7 at%, ● 1 at%, ▼ 1.7 at%, ○ 2.0 at%)

cesses like variable range hopping [14]. The barrier height (E_B) has been evaluated from the data in the high-temperature region. E_B thus obtained has been plotted as a function of carrier concentration n in Fig. 8. There is a decreasing tendency of the magnitude of barrier height (E_B) with increase in n. In Table 1 we have noted the electrical transport parameters at room temperature for all the samples.

The barrier heights obtained in this case are slightly higher than those of doped polycrystalline Si films (33.5 to 5 meV) [10] and are consistent with the previously reported value [15]. In the following section the grain boundary model of Seto [10], later modified by Baccarani et al. [16], for calculating barrier height and carrier concentration in polycrystalline silicon film has been adopted to explain our experimental data.

The details of Seto's theory and the modification introduced by Baccarani et al. [16] are available in the literature. According to Seto, in a polycrystalline material there are a large number of trapping states at the grain boundary. They immobilize the carriers that are charged causing a barrier and reducing the mobility. Seto's theory does not include the possibility that the acceptor states are partially filled when the depletion region does not extend throughout the entire crystallite. Baccarani and others have included this possibility and also assumed both δ-shaped and uniform energy distribution of interface states at the grain boundary. Assuming N_t acceptor states with energy E_t referred to the intrinsic Fermi level at the interface one has to solve electrical neutrality condition across the barrier and the Poisson equation. The resultant equations can be solved by an iterative procedure for the barrier height E_B. For a given crystallite

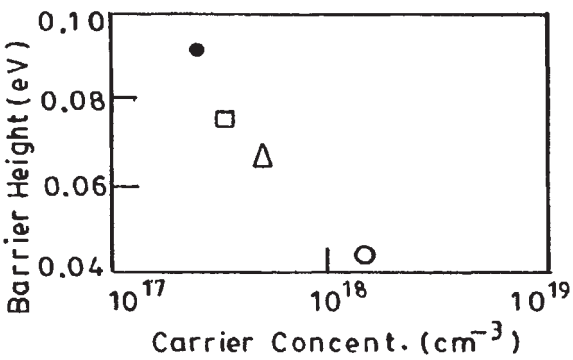

Fig. 8. Plot of barrier height (E_B) against carrier concentration (n) at room temperature of different doped films (● 0.7 at%, □ 1 at%, ○ 1.7 at%, △ 2 at%)

Table 1
The various electrical transport parameters of different aluminum-doped films at room temperature

doping concentration n_d (at%)	carrier concentration n (10^{17} cm^{-3})	resistivity ϱ (Ω cm)	Hall mobility μ (cm^2/V s)	barrier height, E_B (meV)	acceptor states at the g.b., N_t (10^{12} cm^{-2})
0.7	2.58	6.62	3.65	91.0	
1.0	3.4	5.05	3.64	75.0	
1.7	15.0	0.476	8.7	44.0	1.1
2.0	5.0	3.6	3.47	67.0	
0.7*)	108	0.076	7.61		
1.7*)	120	0.010	52.08		

* These samples were heated at 400 °C for 30 min at high vacuum.

size there exist two possible conditions depending on the carrier concentration, i.e., whether the crystallites are entirely depleted or partially depleted.

When n, the carrier concentration is such that the grains are entirely depleted, then equation for barrier is

$$E_B = e^2 L^2 n / 8\varepsilon\,, \tag{6}$$

where ε is the dielectric constant ($\varepsilon = \varepsilon_r \varepsilon_0$).

When n is such that the crystallites are partially depleted, the barriers are represented by two equations, depending on the position of Fermi level, given by

$$E_B = e^2 N_t^2 / 8\varepsilon n \quad \text{for} \quad E_F - E_t - E_B \gg kT\,, \tag{7}$$

$$E_B = E_g/2 - E_t + kT \ln\{qn^{1/2} N_t / [N_C (2\varepsilon E_B)^{1/2}]\} \quad \text{for} \quad E_F - E_t - E_B \ll kT\,, \tag{8}$$

where E_g is the band gap and E_F is the Fermi energy referred to the intrinsic Fermi level in the neutral region, and N_C is the effective density of states at the conduction band. In Fig. 9 there is a plot of barrier height versus carrier concentration for a grain size of 40 nm with different values of N_t. The computer simulated diagram fitting the

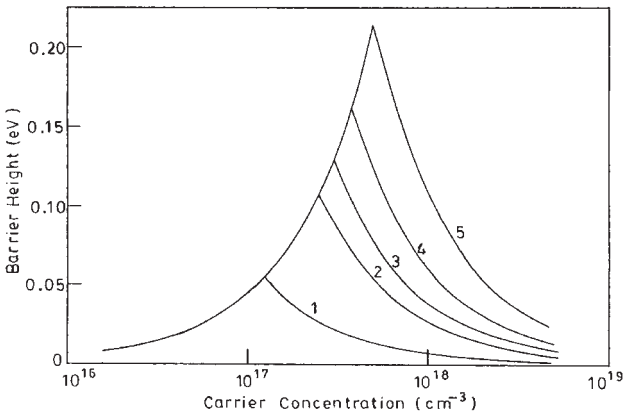

Fig. 9. Nature of simulated barrier height (E_B) against carrier concentration (n) at different values of density of trapped states (N_t): (1) 5.0×10^{11}, (2) 1.0×10^{12}, (3) 1.2×10^{12}, (4) 1.5×10^{12}, (5) 2.0×10^{12} cm^{-2}, corresponding to grain size of 40 nm

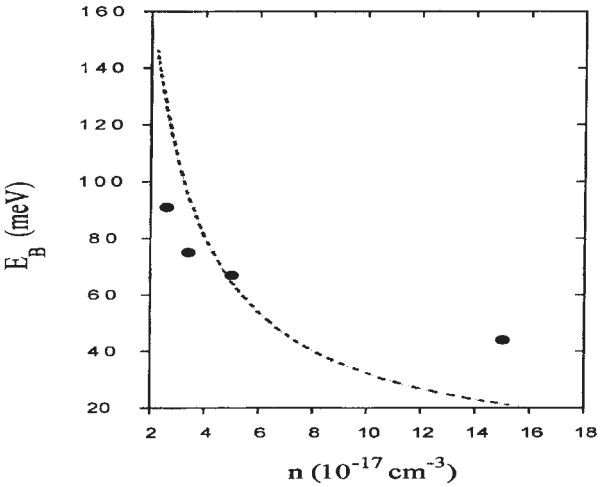

Fig. 10. Plot of experimental data (●) and simulated curve (dotted line) of barrier height (E_B) against carrier concentration (n) at an average value of density of trapped states $N_t = 1.1 \times 10^{12}\,\mathrm{cm}^{-2}$ through the experimental data

experimental values of barrier height to the appropriate value of N_t ($N_t = 1.1 \times 10^{12}\,\mathrm{cm}^{-2}$) is shown in Fig. 10. The experimental data do not fit very well to the theoretical curve corresponding to that particular value of N_t. The deviation is pronounced in the region where barrier height is lower and carrier concentration is higher. Admittedly there is limitation to the above interpretation for Eqs. (7) and (8) are too simplified as they do not take into account of grain size variation or other than monovalent trapping. Nevertheless, an average value of the density of trapped states at the interface can be estimated.

The conductivity in ZnO is due to conduction through electrons created by oxygen vacancy and/or zinc interstitial atoms. The conductivity due to Al^{3+} ion substitution in the sites of Zn^{2+} ion, or Al interstitial, zinc interstitial atom and oxygen vacancies are the probable causes of conduction through electrons for aluminum-doped samples. From Table 1 and Fig. 4 it can be seen that carrier concentration and mobility increase with Al doping reaching a maximum value at 1.7 at%-doped samples. Further doping does not improve the conductivity. Moreover, as already mentioned, carrier concentration is much less than the doping concentration. This suggests that not all the Al atoms in the film contribute as dopants. The films prepared by the other methods, like rf magnetron sputtering [17], also indicated similar results. The decrease in carrier concentration can be explained as due to segregation of aluminum atoms at the grain boundary or trapping of charge carriers by the trapping states at the g.b. In the case of silicon, Baccarani et al. [16] showed that both of these two are taking place simultaneously, which might hold good in this case also. The decrease in mobility μ after doping above 1.7 at% is due to scattering from grain boundaries and ionized impurities,

$$1/\mu = 1/\mu_i + 1/\mu_g\,, \tag{9}$$

where μ_i and μ_g are the mobilities due to impurity scattering and g.b. scattering, respectively. As impurity concentration increases there should be some decrease in μ due to ionized impurity scattering. But initially the height of the potential barrier decreases with carrier concentration (Fig. 8) thereby increasing μ. The rapid decrease in μ thereafter is due to increased g.b. scattering. Nevertheless, following Bellingham et al. [18]

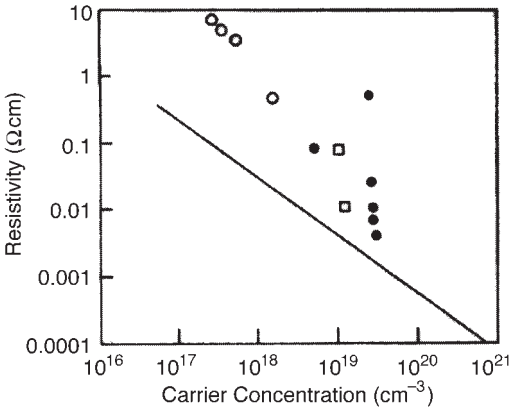

Fig. 11. Plot of resistivity against carrier concentration. The theoretical limiting value is shown as solid line. The experimental values are shown as a) present experiment (○); b) after vacuum heating of our samples (□); c) other sol–gel process (●)

we can set a lower limit of resistivity that can be achieved considering only the Coulomb interaction between ionized donor impurity and the free electrons in a doped material. In actual cases there are presence of neutral impurities and defects and structural disorder. A simple calculation simulates the lower resistivity curve, which is shown in Fig. 11 as a solid line. Our experimental points are also shown in the same figure. We have also introduced some experimental data by others on samples prepared by the sol–gel technique. There are also two points for samples heat-treated in vacuum at 400 °C (Table 1). E_b could not be calculated for vacuum-treated samples, as the resistivity changes with temperature were not performed. Agreement with the lower limit value obviously is better as carrier concentration increases because the scattering from non-ionized impurities becomes more prominent as n decreases.

4. Conclusions

(i) The AZO films prepared by the sol–gel method are conducting and transparent. The carrier concentrations are found to be several orders less than the doping concentration, indicating thereby that the impurities are not sufficiently ionized to take part in the conduction. This might be due to both segregation of impurity atoms at g.b. and trapping of ionized impurities at the trapped states. However, the conductivity is increased by two orders of magnitude if heated in high vacuum.

(ii) There is an increase in carrier concentration and mobility up to 1.7 at%-doped films and further doping is not favorable to produce better conducting films.

(iii) The experimental data has been examined in terms of the grain-boundary-trapping model using uniform energy distribution of interface states. Although the experimental data does not fit exactly the theoretical curve an average value of the density of trapping states at the interface can be predicted. In this case, the average value of $N_t = 1.1 \times 10^{12}\,cm^{-2}$.

(iv) The curve on a lower limit of resistivity against carrier concentration considering only the presence of ionized donor impurity indicates that the number of non-ionized impurities increases as carrier concentration decreases.

References

[1] P. Soubtte, S. Bethke, B. W. Wessels, and H. Pan, J. Cryst. Growth **86**, 248 (1988).
[2] M. F. Ogawa, Y. Natsume, T. Hirayama, and H. Sakata, J. Mater. Sci. Lett. **9**, 135T (1990).

[3] T. MINAMI, H. NANTO, S. SHOOJI, and S. TAKATA, Thin Solid Films **111**, 167 (1984).
[4] T. MINAMI, H. NANTO, and S. TAKATA, Thin Solid Films **124**, 43 (1985).
[5] P. WU, Y. M. GAO, J. BAGLIO, R. KERSHAW, K. DURIGHT, and A. WOLD, Mater. Sci. Bull. **24**, 905 (1989).
[6] F. CALLIUD, A. SMITH, and J. BOUMARD, J. Eur. Ceram. Soc. **6**, 313 (1990).
[7] Y. OHYA, H. SAIKI, and T. TAKAHASHI, J. Mater. Sci. **29**, 4099 (1994).
[8] M. OHYAMA, H. KOZUKA, and T. YOKO, J. Am. Ceram. Soc. **81**, 1622 (1998).
[9] A.L. FRIPP, J. Appl. Phys. **46**, 1240 (1975).
[10] J. Y. W. SETO, J. Appl. Phys. **46**, 5247 (1975).
[11] J. VOLGER, Phys. Rev. **79**, 1023 (1950).
[12] R. L. PETRIZ, Phys. Rev. **104**, 1508 (1956).
[13] J. W. ORTON and M. L. POWELL, Rep. Prog. Phys. **43**, 1263 (1980).
[14] Y. NATSUME, H. SAKATA, T. HIRAYAMA, and H. YANAGIDA, J. Appl. Phys. **72**, 4203 (1992).
[15] T. TSURUMI, S. NISHIZAWA, N. OHASHI, and T. OHGAKI, Jpn. J. Appl. Phys. **38**, 3682 (1999).
[16] G. BACCARANI, B. RICCO, and G. SPADINI, J. Appl. Phys. **49**, 5565 (1978).
[17] K. H. KIM, K. C. PARK, and D. Y. MA, J. Appl. Phys. **81**, 7764 (1997).
[18] J. R. BELLINGHAM, W. A. PHILLIPS, and C. J. ADKINS, J. Mater. Sci. Lett. **11**, 263 (1992).